^{31}P-Magnetic resonance spectra of ovarian cancer cells exposed to chemotherapy within a three-dimensional Matrigel construct

YORAM ABRAMOV[1], SHANI CARMI[2], JACK S. COHEN[2], SHAOUL O. ANTEBY[3] and ISRAEL RINGEL[2]

[1]Department of Obstetrics and Gynecology, Carmel Medical Center, Technion University, Rappaport Faculty of Medicine, Haifa, Israel; Departments of [2]Pharmacology and [3]Obstetrics and Gynecology, Hadassah Hebrew University Medical School, Jerusalem, Israel

Received March 6, 2012; Accepted April 23, 2012

DOI: 10.3892/or.2012.1810

Abstract. We aimed to determine the metabolic profile and effects of chemotherapy on ovarian cancer cell metabolism in a three-dimensional (3D) vs. a two-dimensional (2D) construct using ^{31}P-magnetic resonance spectroscopy (MRS). Three ovarian cancer cell lines were embedded in a 3D perfused Matrigel construct or grown in a 2D monolayer. Metabolic differences between the three cell lines were determined using ^{31}P-MRS both in the 3D and in the 2D constructs. Cells were incubated with three different cytotoxic drugs at LC_{50} for 44 h and evaluated for metabolic changes using ^{31}P-MRS. While the 3D construct allowed MRS assessment of viable cells, the 2D monolayer permitted evaluation of non-viable cell extracts. In both cells embedded in Matrigel (CEM) and cells grown in monolayers (CGM) different cancer cell lines showed characteristic metabolic fingerprints, which differed significantly between CEM and CGM. In contrast to the cell monolayer, CEM allowed continuous monitoring of the changes in ^{31}P-MRS spectra over time following exposure to chemotherapy, demonstrating a progressive decrease in specific phosphorylated metabolites. The metabolic response of CEM and CGM to various antimitotic agents was significantly different. We conclude that different ovarian cancer cell lines show characteristic ^{31}P-MRS fingerprints and specific metabolic changes in response to cytotoxic drug treatment. The perfused 3D Matrigel construct is superior to the 2D tissue monolayer for ^{31}P-MRS studies, because it simulates the *in vivo* conditions more closely and facilitates MRS evaluation of viable cells as well as continuous monitoring of metabolic changes in response to chemotherapy over time.

Correspondence to: Dr Yoram Abramov, Department of Obstetrics and Gynecology, Carmel Medical Center, Technion University, Rappaport Faculty of Medicine, Haifa, Israel
E-mail: yabramov@012.net.il

Abbreviations: ^{31}P, phosphorus-31; ADP, adenosine diphosphate; ATP, adenosine triphosphate; CEM, cells embedded in Matrigel; CGM, cells grown in monolayers; ER, estrogen receptor; GPC, glycerophosphocholine; GPE, glycerophosphoethanolamine; MHz, megaHertz; MRS, magnetic resonance spectroscopy; NADP, nicotine adenine diphosphate; NMR, nuclear magnetic resonance; PBS, phosphate-buffered saline; PCr, phosphocreatine; PC, phosphorylcholine; PCA, perchloric acid; PDE, phosphodiesters; Pi, inorganic phosphate; PME, phosphomonoesters; PtdC, phosphatidylcholine; UDPS, uridine diphospho-sugar; PtdE, phosphatidylethanolamine; PtdI, phosphatidylinositol; PtdS, phosphatidylserine;

Key words: carboplatin, cisplatin, cytotoxic drugs, magnetic resonance spectroscopy, Matrigel, ovarian cancer, phospholipid metabolites, paclitaxel

Introduction

Although epithelial ovarian cancer accounts for 3% of cancers in women, it is the leading cause of death from gynecological cancer and the fifth leading cause of all cancer-related deaths among women in the USA (1). Due to the invasive nature of these tumors and the current inability to detect the disease at early stages, a significant number of women are initially diagnosed only after the neoplasia has spread throughout the peritoneal cavity (2). Consequently, despite advancements in surgical debulking techniques, optimization of chemotherapeutic regimens, and improvements in radiotherapy, 5-year progression-free survival and overall survival rates remain low (3,4). Accurate and reliable diagnostic means are essential to improve the outcome of these patients. The genetic events that are associated with carcinogenesis are often accompanied by metabolic alterations. A technique that may discover biochemical features associated with the malignant changes may be an important tool for ovarian cancer research.

Magnetic resonance spectroscopy (MRS) technology is a relatively novel technique which has been developed over the past five decades. It monitors radiofrequency-induced transitions between the spin states of atomic nuclei in an external magnetic field, and is currently used to provide physiological and biochemical information about cells and tissues *in vitro* and *in vivo*. The development of solenoidal coils has allowed non-invasive, high-resolution ^{31}P-MRS of both animal and human tumors *in vivo* (5-7). ^{31}P-MR spectra primarily provide information about lipid and high energy phosphate metabolism, which may be used clinically in the prediction and monitoring of tumor treatment response (8-10). Moreover,

the ability to follow the cell metabolism pattern in malignant cells, before and after drug treatment, may assist in predicting treatment success. In our previous study we applied ^{31}P-MRS to *in vitro* studies of various breast cancer cells grown in culture, and observed the effects of the drugs on the cells (11). Only a few MRS studies have been reported on human ovarian pathologies, essentially confined to the analysis of fluids from ovarian cysts. From these analyses, significant differences in a variety of soluble metabolite concentrations (some still unassigned) were found between benign and malignant ovarian cysts (12,13).

While cancerous tissues or animal models have been frequently used to study tumor behavior, these approaches are sometimes complex and intractable, presenting challenges for interpreting discrepancies (14) in addition to other difficulties and costs dealing with tissues and animals. On the other hand, traditional 2D cell culture, the widely used standard monolayer culture for cancer cells, provides few physiological resemblance of a tumor growth environment *in vivo* attributed from morphology, cell-cell and cell-matrix interactions. To fill in the gap between the monolayer cell culture and whole animal, the 3D *in vitro* culture has emerged as a third approach that mimics the *in vivo* cell growth environment. Three-dimensional tumor models have emerged as valuable *in vitro* research tools, though the power of such systems as quantitative reporters of tumor treatment response has not been adequately explored. The goal of the 3D culture is to permit researchers to investigate the cellular mechanisms and effects of antitumor agents in conditions resembling those found *in vivo* (14,15) while taking advantage of *in vitro* culture's simplicity and low cost (as opposed to the tissues/animals' complexity, intractability and high cost). In the current study we aimed to determine the metabolic profile and the effects of chemotherapy on several human ovarian cancer cell lines in a perfused 3D vs. a 2D construct using ^{31}P-MRS. Based on our knowledge in this field (16), we hypothesized that for optimal experimental purposes, perfused 3D cell constructs represent a superior model. They provide a metabolically stable and homogeneous environment which resembles the *in vivo* conditions more closely, and is therefore more appropriate for studying cellular mechanisms.

Materials and methods

Human ovarian cancer cell lines. Three human ovarian carcinoma cell lines were used for this study: OC238, an ovarian carcinoma cell line of epithelial origin obtained from malignant ascites. It was histopathologically determined as serous cystadenocarcinoma and was immunohistologically stained for the CA-125 marker. Its tumorigenic nature was determined by injection of the established *in vitro* cultures to nude mice and the creation of growing tumors (17). The A2780 (ECACC No. 93112519) ovarian adenocarcinoma cell line was established from tumor tissue from an untreated patient. The A2780cisR (ECACC No. 93112517) cisplatin-resistant cell line has been developed by chronic exposure of the parent cisplatin-sensitive A2780 cell line to increasing concentrations of cisplatin. A2780cisR is cross-resistant to melphalan, doxorubicin and irradiation. An increased ability to repair DNA damage as well as cytogenetic abnormalities have been observed in this cell line (data from ECACC). All cell cultures were grown in DMEM supplemented with 10% FCS, 1% sodium pyruvate solution 100 mM, 1% L-glutamine solution 200 mM, 1% MEM-vitamins solution 100X, 1% MEM-non-essential amino acids solution 100X and 1% penicillin-streptomycin solution (Biological Industries, Israel). The two cell lines, A2780 and A2780cisR were also supplemented with bovine insulin solution 10 mg/ml (Sigma) diluted to 10 μg/ml. Cell cultures were grown either in 92x17-mm dishes for further culturing or in 144x21-mm dishes (Nunclon) when larger amounts of cells were required. Cultures were regularly fed every 3-4 days and sub-cultured by a 1:30-40 split ratio by detaching cells after one PBS wash with trypsin (0.05%) EDTA (0.02%) solution (Biological Industries). Cultures were occasionally frozen in fresh medium containing 10% DMSO. A2780cisR cells which had a higher rate of growth than the other two cell lines, were split in higher dilutions (1:50-1:70). All cultures were incubated at 37˚C with 5% CO_2.

Three-dimensional Matrigel construct. In order to follow changes occurring in living cells using the MRS technique, the cells were packed in the MRS tube in Matrigel (BD Matrigel™ Matrix, BD Biosciences, USA), a solubilized basement membrane preparation extracted from EHS mouse sarcoma, (a tumor rich in ECM proteins) whose major components are laminine (56%), followed by collagen IV (31%), heparan sulfate proteoglycans, and entactin (8%). At room temperature, Matrigel polymerizes to produce biologically active matrix material resembling the mammalian cellular basement membrane. Prior to the procedure, Matrigel was thawed at 4˚C in an ice-water bath, a flask was filled with 60 ml of fresh medium either with or without drugs, and a 60-cm long teflon tube of 0.5 mm inner diameter was attached to a sterile 23G needle on a 10-ml syringe. The tube was washed twice with 70% ethanol and the whole apparatus was kept in ethanol until it was used. For each experiment 3 dishes of 144x21-mm were cultured to full confluency. Cells were detached using trypsin and centrifuged for 5 min at 1,000 rpm. The medium was removed and the tube containing the cells was set on ice in a box, which was earlier sterilized with ethanol. Cold (4˚C) Matrigel (1.5 ml) was added to the cells using a cold sterile pipette. The cells and the Matrigel were gently mixed into a homogenous suspension. Matrigel threads were then prepared one after the other as quickly as possible in order to place the cells back into the medium rapidly. The suspension was gently drawn into the teflon tube and was left in the tube at room temperature for 30-120 sec until it polymerized. The teflon tube was occasionally cleaned with a tissue soaked in ethanol and then the thread was pushed out of the tube and into the flask containing the medium. After the whole suspension was transformed into semi-solid threads, the cells were left to incubate in the medium for about 30-33 h in the incubator at 37˚C, 5% CO_2.

Perfusion system. For the MRS analysis, Matrigel threads containing the ovarian cancer cells were transferred to the 10-mm sterilized MRS tube attached to a perfusion system activated by a peristaltic pump. The system allowed constant perfusion of fresh medium to the threads, while the Matrigel was holding the cells. Prior to the experiments the tubing was washed with ethanol and then with the medium. After

attaching the tube to the system, the pump was turned on and the medium was constantly replaced during the experiment at a rate of 0.5 ml/min. A mixture of 95% O_2 and 5% CO_2 was bubbled into the medium to assure the viability of the cells. MRS analysis of the living CEM was conducted overnight and the total incubation time of the cells in the Matrigel was about 45 h. A set of experiments was performed with each cell line. At least two experiments were performed without any drug, as control, followed by the chemotherapeutic experiments for each cell line with each drug. The concentrations of drugs added to the media for the experiments in living CEM were 10 times higher than the LC_{50} values for CGM, as previously reported (11).

Determination of cell growth in Matrigel. Cells were embedded in Matrigel threads in several concentrations depending on the cell line proliferation profile. Every 24 h, threads were extruded into Petri dishes containing 10 ml of medium and placed in an incubator. At each time point, two threads were dissolved in Matrisperse (for 1 h on ice). The number of cells was determined by a homocytometer.

The two-dimensional cell monolayer construct. A common method for characterization of the intracellular components of cell monolayers is by extracting tissues and cells and conducting MRS detection of the solubilized extracts. Perchloric acid extracts enable detection of water-soluble metabolites such as amino acids, sugars and phospholipids. Chloroform/methanol extracts allow characterization of lipophilic compounds, such as membrane phospholipids. These extracts produce homogenous solutions that generate highly resolved spectra and allow detection of metabolites of low concentrations. In order to have a sufficient amount of material for the MRS analysis a ~$3x10^8$ cells were extracted for each sample. To reach this number, cells were cultured in 3 dishes of 144x 21-mm size and were extracted only when the dishes were fully confluent. Cells were detached using the trypsin-EDTA solution and were collected in a 50-ml tube for centrifugation for 5 min at 1,000 rpm. The supernatant was removed and 1 ml of $HClO_4$ 0.5 M was added to the tube which was kept on ice during the whole procedure. The incubation in perchloric acid lasted 5 min and the solution was occasionally mixed by vortexing. The acid was then neutralized to pH 7.0 using KOH and was centrifuged for 15 min at 10,000 rpm (4˚C). The supernatant was transferred to a 20-ml plastic bottle and was mixed with 0.2 g Chelex 100 (Bio-Rad Laboratories, Hercules, CA, USA) for 1 h at 4˚C. The solution was then filtered through a GF/B (1.0 μM pore size) 2.5 cm diameter Glass Microfibre filter (Whatman, UK) into a 150-ml glass flask. The filter was washed with cold double-distilled water (DDW) before and after filtration. The filtrate was frozen in liquid nitrogen and lyophilized overnight until dried. The dry sample was kept sealed in the flask, at -80˚C until analysis.

Antimitotic drugs. Three antimitotic drugs were used: paclitaxel (Taxol, Bristol-Myers Squibb, USA), cisplatin (Vianex, Greece) and carboplatin (Paraplatin; Bristol-Myers Squibb, Italy). Stock concentrations of the drugs were: paclitaxel 6 mg/ml, cisplatin 1 mg/ml and carboplatin 10 mg/ml. Paclitaxel was further diluted in DMSO and the platinum compounds were diluted in DDW. In order to determine the effective concentrations of the drugs to be used with the cell cultures, a series of experiments were conducted to determine the LC_{50}. The following procedure was performed at least twice with each cell line. Cells were seeded in a 12-well plate (6 duplicates) at 10,000 cells/ml at 2 ml/well. About 24 h after seeding the drug was added to five of the six duplicates in increasing concentrations. Two wells were left untouched, as controls. The middle concentration was close to the estimated LC_{50}, two duplicates had higher concentrations and two had lower. The volume of the drug solution, which was added to the well, was never >1% of the total volume. After 48 h of incubation with the drugs, the wells were washed with PBS in order to wash away dead cells and the adherent cells were detached using trypsin. The cells were transferred to a cuvette and diluted in PBS to a total volume of 20 ml. Cells were counted in a Coulter Counter®, (Beckman Coulter) which was calibrated to the proper size of particles after a sample manual counting. Each cuvette was counted four times and all counts were compared to the control count of the clean PBS. Counting results were analyzed using Microsoft Excel and the derived LC_{50} parameters were used in the chemotherapeutic experiments.

Magnetic resonance spectroscopy. The dry extracts were disolved in 700 μl cold D_2O, mixed and moved to a 1.5 ml eppendorf tube for 10-min centrifugation at 10,000 rpm. D_2O enables the lock signal on the nuclear magnetic resonance (NMR) machine to be used. The solution was then transferred to a 5-mm NMR tube and was kept at 4˚C until analysis. Before MR analysis for ^{31}P containing compounds, 70 μl of EDTA solution (0.2 M) was added to the NMR tube to remove paramagnetic ions. Samples were constantly kept on ice. Most of the MR experiments were performed on the Varian Inova 500 machine that detects ^{31}P-nuclei at 202 MHz. Prior to each series of experiments, the values of T_1 and the required 90º pulse width (pw) were determined and then used for the analysis. MR experiments of all extracts were carried out using the 5BB probe at 10˚C. The spectometer frequency (sfrq) was set at -202.319 MHz for the ^{31}P detection. Parameters were set: transmitter power (tpwr) of 56; pw of 7.0 μsec, (flip angle of 66.3º); d1 of 2.00 sec; at of 1.60 sec. Broad-band decoupling was activated to suppress the proton detection: dn, 1H; dpwr of 40; dm=y; dmm=w. Scans (n=3,000) were accumulated to produce the final spectrum. All spectra were analyzed with the MestRe-C software version 3.6.9. Processing included line broadening of 2.00, and manual or auto phasing where necessary. Spectra were manually integrated by marking the beginning and ending of each signal of interest. The first signal marked was automatically set as 1 and all other referred to it. The signal of β-ATP at -21 ppm was set as a reference. All integrals of all signals were set in tables in Microsoft Excel spreadsheets. The averages and standard deviations were calculated where the database was sufficient, using functions of the Microsoft Excel software. Figures were created using Microsoft Excel.

The main phosphorus-containing metabolites that are present in the ^{31}P-NMR spectra of cells are phosphomonoesters (PME), phosphorylcholine (PChol) and phosphorylethanolamine (PEtn) that are the substrates for the biosynthesis of phosphatidylcholine (PtdCho) and phos-

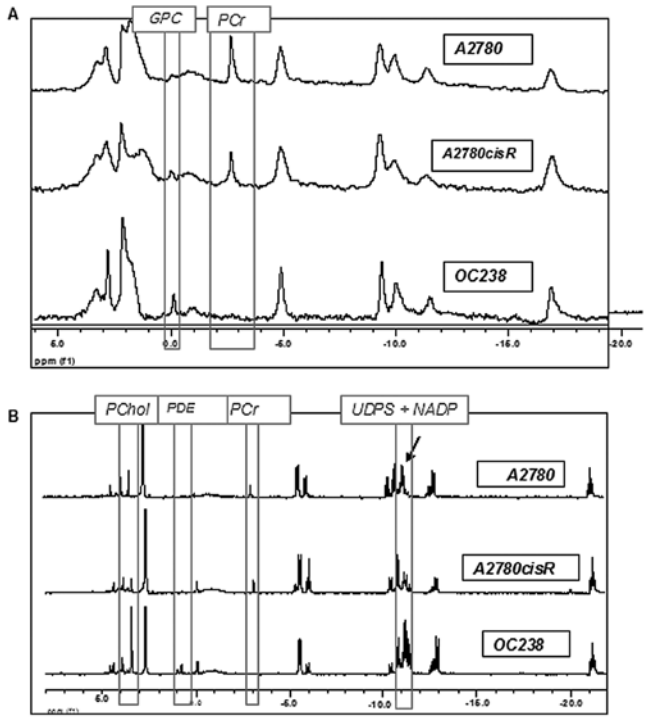

Figure 1. ^{31}P-MR spectra of three different ovarian cancer cell lines. (A) Performed in viable cell cultures embedded in Matrigel. (B) Performed in cell extracts. Significant differences between the three cell lines are marked by the grey boxes.

phatidylethanolamine (PtdEtn), respectively. PtdCho is the major phospholipid component of eukaryotic cells, involved in membrane structure, signal transduction and lipoprotein metabolism. PtdEtn is one of the other phospholipids forming cellular membranes. PtdCho can be broken down by a specific phospholipase C to produce diacylglycerol which is an important second messenger in many cellular metabolic pathways. Phosphodiesters (PDE) include glycerophosphocholine (GPC) and glycerophosphoethanolamine (GPE). GPC is the product of the complete deacylation of PtdChol and is also the inhibitor (negative feedback) of lysophospholipase which is one of the enzymes responsible for the breakdown of PtdCho. GPC is a precursor in the production of choline that is the precursor for phospholipids and acetylcholine. GPE is a derivative and a substrate in the biosynthesis of PtdEtn (18). Phosphocreatine (PCr) is a highly important molecule in the energetic cycles in the cell. It readily donates a phosphate to ADP in order to produce ATP whenever it is required (19). Uridine diphospho-sugar (UDPS) is a key group of intermediates in carbohydrate metabolism, which serve as precursors for glycogen and can be metabolized into UDP galactose and UDP glucuronic acid which are incorporated into polysaccharides as galactose and glucuronic acid. They also serve as precursors for sucrose lipopolysaccharides, and glycosphingolipids. Nicotinamide adenine dinucleotide phosphate (NADP) is an important oxidizing co-enzyme participating in many anabolic processes (e.g., lipid, amino acid, sugar and nitrogen metabolism) (19).

Statistical analysis. Data are expressed as mean ± SEM. Statistical significance was assessed by a Student two-tailed t-test, and analysis of variance as indicated. A value of $P<0.05$ represents significance compared to untreated controls, unless otherwise indicated.

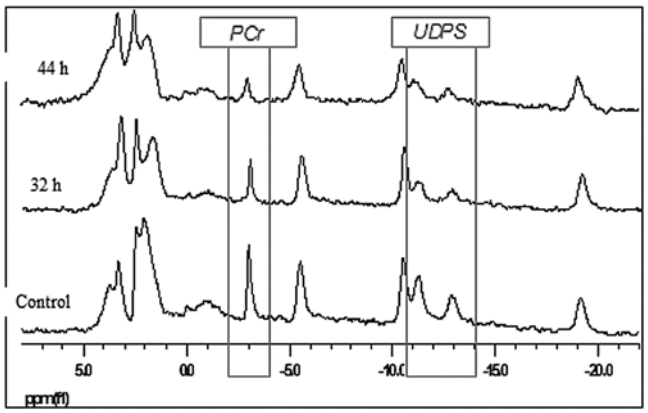

Figure 2. Changes in the ^{31}P-MR spectra of viable A2780 ovarian cancer cells embedded in Matrigel during continuous exposure to cisplatin. Significant differences between the various exposure times and control are marked by the grey boxes.

Results

Characterization of cell lines by MRS. Only experiments in which the levels of β-ATP did not decrease significantly were included in the analysis to assure that the changes observed are due to the chemotherapeutic effect and not to cell death. While the 3D Matrigel construct allowed MRS assessment of viable cells, the 2D monolayer permitted evaluation of non-viable cell extracts only. Significant differences in the ^{31}P-MR spectra could be detected between the different cell lines. As shown in Fig. 1A, the spectra of intact CEM had relatively lower resolution and signal-to-noise ratio compared to the spectra of the extracts, probably due to the non-homogeneity of the samples. In both viable CEM and in cell extracts, A2780 and A2780cisR cell lines had a high phosphocreatine (PCr) signal which was absent in the OC238 cell line (Fig. 1). While viable cells in Matrigel showed only a higher GPC signal in OC238 compared to A2780 and 2780cisR cell lines (Fig. 1A), extracted cells from the monolayer showed higher PChol, PDE, UDPS and NADP signals in the OC238 cell line (Fig. 1B).

Changes in metabolite levels following chemotherapy. The concentration that causes death in 50% of the cells, LC_{50}, was calculated for all three cell lines, either grown in monolayers or embedded in Matrigel. According to our previous data (11), the LC_{50} for CEM was higher by one order of magnitude compared to that of CGM. After the cultures were incubated with the drugs in the LC_{50}, they underwent MRS analysis. In contrast to the CGM, cells grown in the 3D Matrigel construct allowed continuous monitoring of the changes in ^{31}P-MRS spectra following incubation with cytotoxic drugs. The ^{31}P-MRS spectra of the A2780 cell line in living CEM and incubated with cisplatin for 44 h are presented in Fig. 2. Compared to the control specimen whose spectra did not significantly change over time, the PCr and UDPS gradually decreased in response to cisplatin exposure. In order to compare the different samples in a quantitative manner, a common integration method was

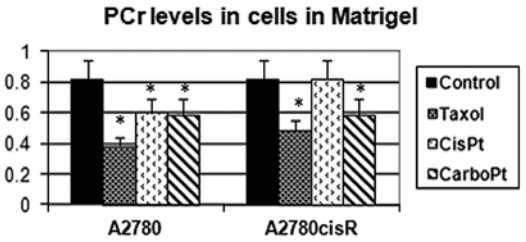

Figure 3. Integrals (normalized to β-ATP) of the ^{31}P-MRS signals in the A2780 and A2780cisR cell lines grown in Matrigel following incubation with different cytotoxic drugs. *P<0.05 for comparisons between the control and drug treatment.

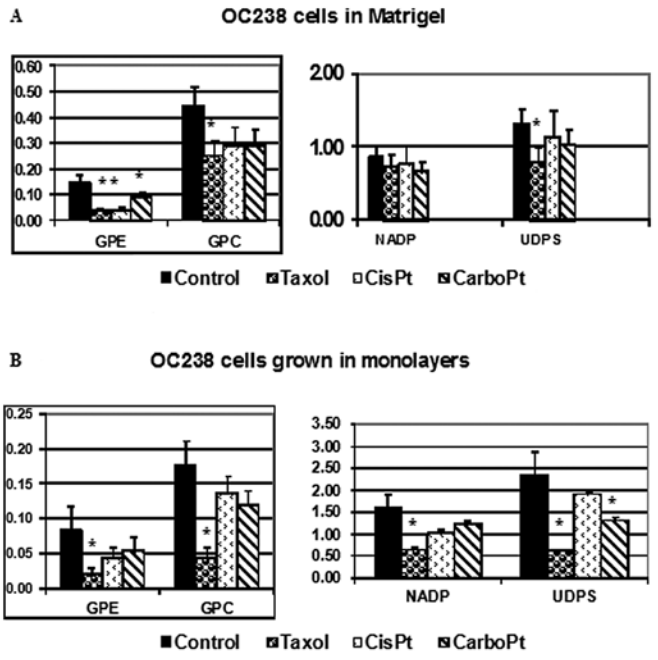

Figure 4. Integrals (normalized to β-ATP) of the ^{31}P-MRS signals in the OC238 cell line following incubation with different cytotoxic drugs. (A) Experiment performed in living ovarian cancer cells embedded in Matrigel. (B) Experiment performed in extracts of cells grown in monolayers. *P<0.05 for comparisons between the control and drug treatment.

used. The intensity of the β-ATP signal was chosen as a reference value since it has been shown to be proportional to the number of cells in the sample and to their state of vitality (prior to extraction). The signal of β-ATP was integrated first and was automatically given the value of one (by the software). All other integrals were calculated relative to it. The integrals of the magnetic resonance spectra of A2780 and A2780cisR (the cisplatin-resistant variant) cell lines grown in Matrigel and exposed to various antimitotic drugs are presented in Fig. 3. While PCr levels decreased in response to all three cytotoxic drugs in the A2780 cell line, they remained unchanged in response to cisplatin in the A2780cisR cell line. Changes in the integrals of magnetic resonance spectra of OC238 cells grown in a perfused 3D Matrigel construct (Fig. 4A) or in monolayers (Fig. 4B), and exposed to various antimitotic drugs were demonstrated. While viable OC238 cells in Matrigel showed a significant decrease in GPE in response to paclitaxel, cisplatin and carboplatin (Fig. 4A), CGM showed a significant decrease in GPE in response to paclitaxel (Fig. 4B). Both OC238 CEM and CGM showed a significant decrease in GPC levels in response to paclitaxel (Fig. 4). While CEM showed no changes in NADP in response to any of the cytotoxic drugs (Fig. 4A), CGM showed a significant decrease in NADP in response to paclitaxel (Fig. 4B). While CEM showed a significant decrease in UDPS in response to paclitaxel, CGM showed a decrease in UDPS in response to both paclitaxel and carboplatin.

Discussion

Ovarian cancer is the leading cause of death in women with gynecological malignancies. For the majority of patients, ovarian cancer is diagnosed at a late stage characterized by disseminated studding of the peritoneal surfaces with tumor nodules ranging in size from microscopic clusters of a few cells to large cakes of disease spanning several centimeters (1,2,20,21). Primary cytoreductive surgery followed by platinum-based chemotherapy is the standard treatment for this cancer. However, the low survival rate despite these treatments, which has improved only marginally over the course of decades, leads to the need for new physiologically relevant research platforms to meaningfully examine treatment response and devise more effective strategies.

Magnetic resonance spectroscopy is a relatively novel technology which enables non-invasive continuous monitoring of biochemical processes. It can detect metabolic alterations associated with malignant phenotypes of cancer cells *in vitro*, as a basis for a possible *in vivo* monitoring of clinical lesions. In particular, ^{31}P-MRS spectra of intact cells and tissues allow detection and quantification of a number of intracellular metabolites and their fluxes in either ubiquitous or tissue-specific biochemical pathways. Among these, particular attention has been devoted to metabolites involved in phospholipid biosynthesis and catabolism (18). ^{31}P-MRS analysis has helped in the understanding of the multidrug resistance mechanism and to distinguish between levels of malignancy and differentiation in neoplastic tissues (16). It has also been used to follow changes occurring in the phospholipid profile of breast cancer cells after addition of precursors such as ethanolamine and choline. We have previously published a ^{31}P-MRS study characterizing different types of breast cancer cells, with a unique fingerprint for each cell line, representing different stages of tumor progression (11). Moreover, ^{31}P-MRS observations revealed a correlation between the mode of action of anticancer drugs and the observed changes in cell metabolic profile.

The study of ovarian cancer by MRS has been limited and performed mainly by proton MRS. One study managed to distinguish ovarian carcinomas from normal and benign tissues, based on alterations of cellular lipid, creatine/PCr, and lysine/polyamines ratios (22). In another study a statistical pattern recognition technique of linear discriminant analysis was used to analyze ovarian cancer biopsy spectra. Using this method, normal and benign samples were distinguished from borderline and malignant samples with a sensitivity of 95% and a specificity of 86%. This method also helped to distinguish between untreated and recurrent ovarian cancer with an overall accuracy of 97%, suggesting that proton MRS can detect chemotherapy-induced changes in ovarian neoplasms

(23). In the current study, the state of phosphate-containing metabolites was recorded for three different ovarian cancer cell lines. The results indicate that different ovarian cancer cell lines show characteristic ^{31}P-MRS fingerprints and specific metabolic changes in response to cytotoxic drug treatment.

The evaluation of newly developed anticancer drugs is usually performed initially in the traditional 2D culture. However, most drugs that are promising in the 2D culture are rarely effective *in vivo* in animals or clinical trials, partially because the clinically relevant tumors do not exist as monolayers *in vivo*. In fact, 2D monolayer cell cultures represent highly reductionist models of epithelial cell cancers, due to the loss of physiological extracellular matrix on artificial plastic surfaces. Consequently, cells lose relevant properties, such as differentiation, polarization, cell-cell communication and extracellular matrix contacts. This imbalance contributes to the poor predictive value of compound efficacies between *in vitro* and *in vivo* experiments. There is no doubt that the development of 3D cultures represents a valuable tool for understanding the pathogenesis of cancer (24,25). Three-dimensional cultures mimic the normal phenotype of epithelial cells *in vivo* and provide a functional and structural environment to investigate the activities of cancer genes. In pioneering studies, the Bissel laboratory established *in vitro* 3D breast cancer models in which normal and malignant breast epithelial cells grown on a bed of growth-factor-reduced GFR Matrigel form polarized 3D acinar structures (26). Matrigel represents a reconstituted, laminine-rich basement membrane, which supports processes such as cell polarity, cell-cell- and cell-matrix interaction, and re-expression of differentiation markers even in transformed lines (27). Implementing these 3D models to understand cell signaling in relation to position within an acinus, their group and others were able to establish basic tumor biology insights into breast carcinogenesis and progression, which would not be possible in monolayer cultures (25,28). While these reports demonstrate the importance of restoring key architectural cues *in vitro*, the full capability of 3D tumor models as a biologically relevant platform for analysis of tumor growth and cytotoxic response has not yet been adequately explored. *In vitro* 3D tumor systems, could be used as tools to provide a window into tumor growth mechanisms *in vivo*, while providing a level of access for imaging and manipulation of the system that is difficult to achieve in animal models. We adopted an ovarian cancer model that draws on the established *in vitro* models of breast cancer in which cells are overlaid on a bed of Matrigel threads. Accordingly, we developed an *in vitro* perfused 3D model which, in conjunction with ^{31}P-MRS allows for a continuous metabolic assessment of perfused viable ovarian cancer cells. The *in vitro* 3D platform of ovarian cancer described here fills a critical niche in translational science by bridging the gap between resource-intensive animal models and traditional monolayer cultures that lack important determinants of tumor growth and treatment response. The 3D perfused Matrigel construct seems to be superior to the 2D tissue monolayer for ^{31}P-MRS studies as it permits continuous MRS monitoring of drug-induced metabolic changes over time. Indeed, the 3D and 2D constructs revealed differences in the fingerprints of the various cancer cell lines as well as different metabolic changes in response to chemotherapy. Treatment response studies have shown that cancer cells induced to form 3D spheroids are vastly less sensitive to chemotherapy than monolayer cells (30). In the current study, the LC_{50} for CEM was higher by one order of magnitude than that of CGM. This cannnot be explained by lower drug penetration through the Matrigel (11). Therefore, the components of the Matrigel or the experimental conditions have some protective action on cancer cells. These data are in accordance with previous studies (31,32), which reported that traditional monolayer cultures significantly overestimate the sensitivity of ovarian cancer cells to cytotoxic treatments, which limits their value as tools to evaluate therapeutic efficacy.

Acknowledgements

This study was funded by the Zaltzberg Research Fund, Hadassah Medical Organization, Israel.

References

1. National Cancer Institute: www.cancer.gov/cancertopics/types/ovarian A snapshot of ovarian cancer. Last updated, October 2011.
2. Jemal A, Siegel R, Ward E, Hao Y, Xu J and Thun MJ: Cancer statistics 2009. CA Cancer J Clin 59: 225-249, 2009.
3. Bast RC, Hennessy B and Mills GB: The biology of ovarian cancer: new opportunities for translation. Nat Rev Cancer 9: 415-428, 2009.
4. Chi DS, Eisenhauer EL, Zivanovic O, *et al*: Improved progression-free and overall survival in advanced ovarian cancer as a result of a change in surgical paradigm. Gynecol Oncol 114: 26-31, 2009.
5. Ng TC and Glickson JD: Shielded solenoidal probe for in vivo NMR studies of solid tumors. Magnet Reson Med 2: 169-175, 1985.
6. Glickson JD, Evanochko WT, Sakai TT and Ng TC: In vivo NMR studies of RIF-1 tumors. In: Magnetic Resonance in Cancer. Allen PS, Boisvert DPJ and Lentie BC (eds). Pergamon Press, Toronto, pp71-82, 1986.
7. Maris JM, Evans AE, McLaughlin AC, D'Angio GJ, Bolinger L, Manos H and Chance B: 31P nuclear magnetic resonance spectroscopic investigation of human neuroblastoma in situ. N Engl J Med 312: 1500-1505, 1985.
8. Evanochko WT, Ng TC, Lilly MB, Lawson AJ, Corbett TH, Durant JR and Glickson JD: In vivo ^{31}P NMR study of the metabolism of murine mammary 16/C adenocarcinoma and its response to chemotherapy, x-radiation, and hyperthermia. Proc Natl Acad Sci USA 80: 334-338, 1983.
9. Okunieff PG, Koutcher, JA, Gerweck L, McFarland E, Hitzig B, Urano M, Brady T, Neuringer L and Suit HD: Tumor size dependent changes in a murine fibrosarcoma: use of in vivo ^{31}P NMR for non-invasive evaluation of tumor metabolic status. Int J Radiat Oncol Biol Phys 12: 793-799, 1986.
10. Ng TC, Evanochko, WT, Hiramoto RN, Chanta VK, Lilly MB, Lawson AJ, Corbett TH, Durant JR and Glickson JD: P NMR spectroscopy of in vivo tumors. J Magnet Res 49: 271-286, 1986.
11. Sterin M, Cohen JS, Mardor Y, Berman E and Ringel I: Levels of phospholipid metabolites in breast cancer cells treated with antimitotic drugs: a ^{31}P-magnetic resonance spectroscopy study. Cancer Res 61: 7536-7543, 2001.
12. Massuger LFAG, van Vierzen PBJ, Engelke U, Heerschap A and Wevers R: 1H-magnetic resonance spectroscopy: a new technique to discriminate benign from malignant ovarian tumors. Cancer 82: 1726-1730, 1998.
13. Boss EA, Moolenaar SH, Massuger LF, Boonstra H, Engelke UF, de Jong JG and Wevers RA: High-resolution proton nuclear magnetic resonance spectroscopy of ovarian cyst fluid. NMR Biomed 13: 297-305, 2000.
14. Yamada KM and Cukierman E: Modeling tissue morphogenesis and cancer in 3D. Cell 130: 601-610, 2007.
15. Ritter CA, Perez-Torres M, Rinehart C, Guix M, Dugger T, Engelman JA, *et al*: Human breast cancer cells selected for resistance to trastuzumab in vivo overexpress epidermal growth factor receptor and ErbB ligands and remain dependent on the ErbB receptor network. Clin Cancer Res 13: 4909-4919, 2007.

16. Cohen J S, Jaroszewski JW, Kaplan O, Ruiz-Cabello J and Collier S: A history of biological applications of NMR spectroscopy. J Prog Nucl Magn Reson Spectrosc 28: 53-85, 1995.
17. Maymon R, Bar-Shira Maymon B, Holzinger M, Tartakovsky B and Leibovici J: Augmentative effects of intracellular chemotherapy penetration combined with hyperthermia in human ovarian cancer cells lines. Gynecol Oncol 55: 265-270, 1994.
18. Podo F: Tumor phospholipid metabolism. NMR Biomed 12: 413-439, 1999.
19. Nakayama S and Clark JF: Smooth muscle and NMR review: an overview of smooth muscle metabolism. Mol Cell Biochem 244: 17-30, 2003.
20. Cho KR and Shih IeM: Ovarian cancer. Annu Rev Pathol 4: 287-313, 2009.
21. Berek JS and Bast RCJ: Ovarian cancer. In: Cancer Medicine. Kufe DW, Pollack RE, Weichselbaum RR, Bast RCJ, Gansler TS, Holland JF and Frei EI (eds). 6th edition. BC Decker, Hamilton, Ontario, pp1831-1861, 2003.
22. Mackinnon WB, Russell P, May GL and Mountford CE: Characterization of human ovarian epithelial tumors (ex vivo) by proton magnetic resonance spectroscopy. Int J Gynecol Cancer 5: 211-221, 1995.
23. Wallace JC, Raaphorst GP, Somorjai RL, Ng CE, Fung Kee Fung M, Senterman M and Smith IC: Classification of ^{1}H MR spectra of biopsies from untreated and recurrent ovarian cancer using linear discriminant analysis. Magn Reson Med 38: 569-576, 1997.
24. Kim JB: Three-dimensional tissue culture models in cancer biology. Semin Cancer Biol 15: 365-377, 2005.
25. Debnath J and Brugge JS: Modelling glandular epithelial cancers in three-dimensional cultures. Nat Rev Cancer 5: 675-688, 2005.
26. Lee GY, Kenny PA, Lee EH and Bissell MJ: Three-dimensional culture models of normal and malignant breast epithelial cells. Nat Methods 4: 359-365, 2007.
27. Streuli CH, Schmidhauser C, Bailey N, *et al*: Laminin mediates tissue-specific gene expression in mammary epithelia. J Cell Biol 129: 591-603, 1995.
28. Debnath J, Mills KR, Collins NL, Reginato MJ, Muthuswamy SK and Brugge JS: The role of apoptosis in creating and maintaining luminal space within normal and oncogene-expressing mammary acini. Cell 111: 29-40, 2002.
29. Ohmori T, Yang JL, Price JO and Arteaga CL: Blockade of tumor cell transforming growth factor-beta enhances cell cycle progression and sensitizes human breast carcinoma cells to cytotoxic chemotherapy. Exp Cell Res 245: 350-359, 1998.
30. Ruiz-Cabello J, Berghmans K, Kaplan O, Lippman ME, Clarke R and Cohen JS: Hormone dependence of breast cancer cells and the effects of tamoxifen and estrogen: ^{31}P NMR studies. Breast Cancer Res Treat 33: 209-217, 1995.
31. Pike MC, Kredich NM and Snyderman R: Influence of cytoskeletal assembly on phosphatidylcholine synthesis in intact phagocytic cells. Cell 20: 373-379, 1980.